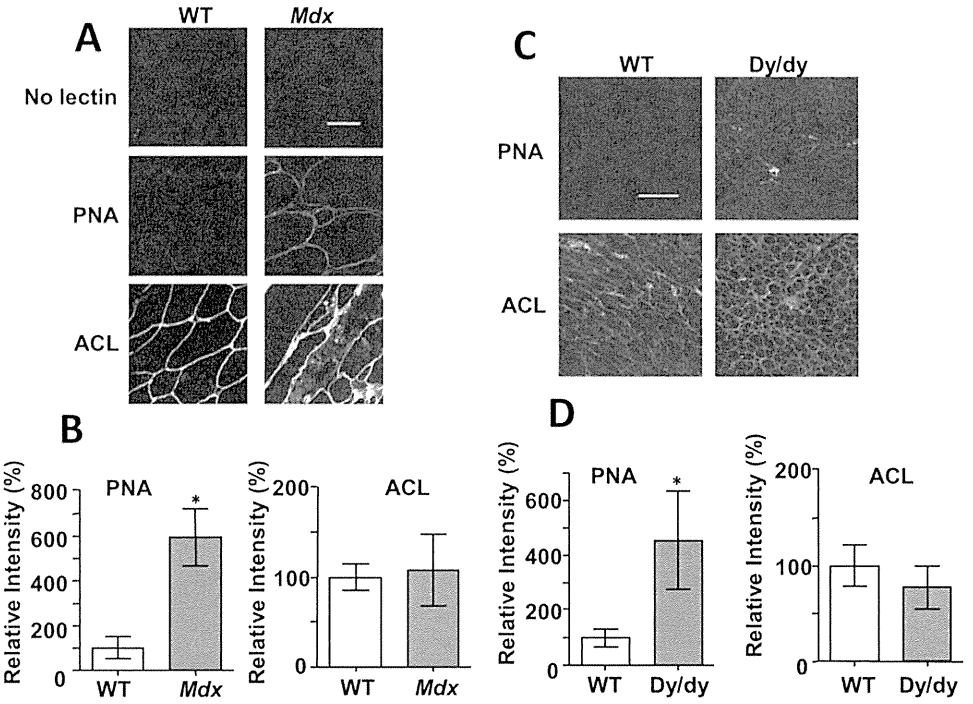

FIGURE 2. Increased PNA staining in the muscles of *mdx* and *dy/dy* mice. (**A**) Frozen sections of quadriceps femoris muscle from *mdx* (*Mdx*) and control mice (WT) were stained with biotinylated PNA or ACL followed by FITC-avidin D. Scale bars: 50 μm. (**B**) Immunofluorescence images of myofiber cross-sections stained with lectins were analyzed by imaging software, and fluorescence intensity was normalized to that of healthy mice. The data are presented as mean ± SD (n = 20–50 fibers/group); *$P < 0.05$. (**C**) Frozen sections of quadriceps femoris muscle from *dy/dy* (*Dy/dy*) and control mice (WT) stained with biotinylated PNA or ACL, followed by FITC-avidin D. Scale bars: 50 μm. (**D**) Immunofluorescence images of myofiber cross-sections stained with lectins were analyzed by imaging software. Fluorescence intensity of each lectin staining was measured from 3 or 4 cross-sectional views of myofibers from 3 or 4 animals per group and normalized to that of healthy mice. The data are presented as mean ± SD (n = 40–50 fibers/group). *$P < 0.05$.

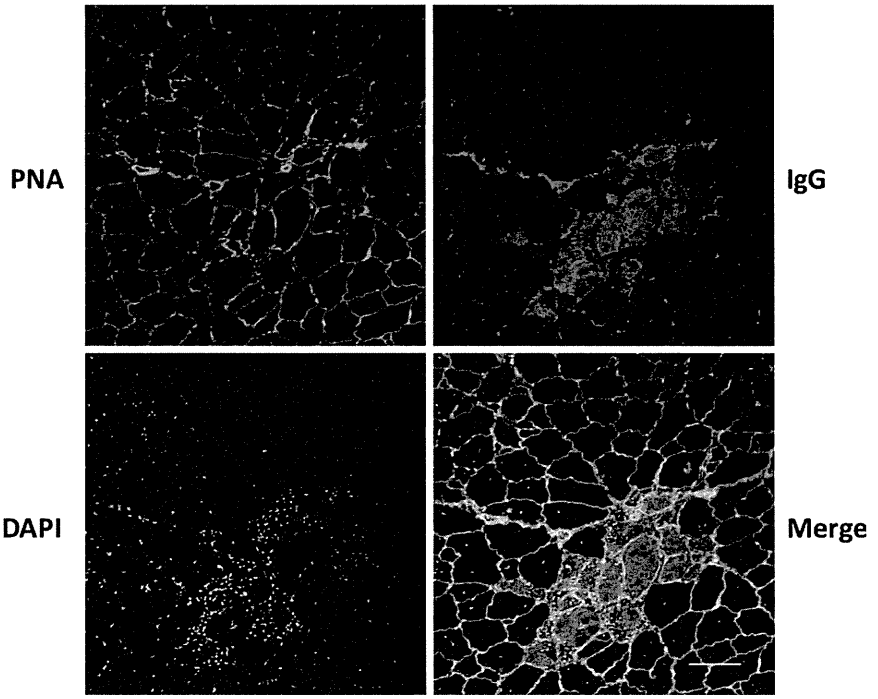

FIGURE 3. PNA staining is observed in all states of muscles, including necrotic fibers. Frozen sections of quadriceps femoris muscle from *mdx* mice were stained with FITC-PNA for sialic acids, DAPI for nuclei, and anti-mouse IgG for necrotic fibers. Scale bars: 50 μm. [Color figure can be viewed in the online issue, which is available at wileyonlinelibrary.com.]

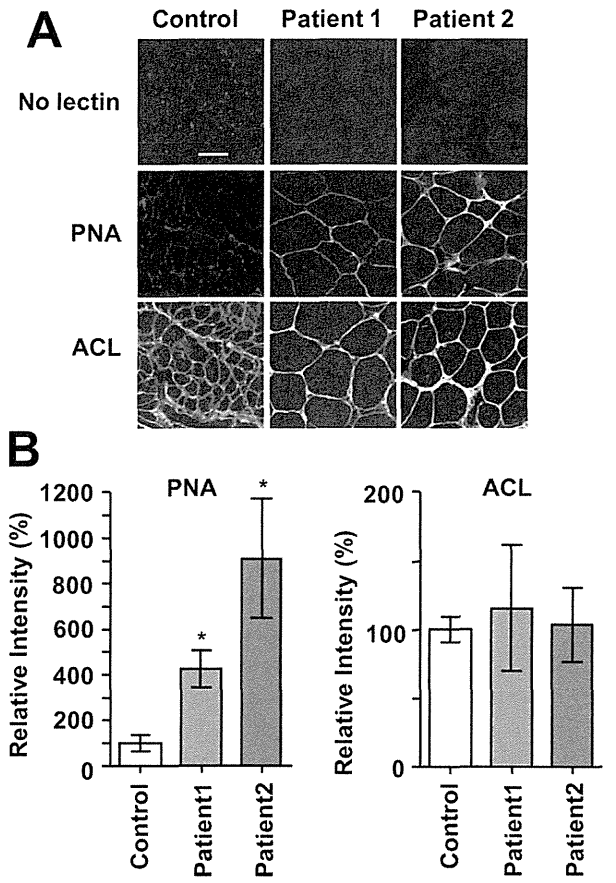

FIGURE 4. Increased PNA staining in the muscles of patients with muscular dystrophy. (**A**) Frozen sections of skeletal muscle from dystrophic patients and non-dystrophic controls stained with biotinylated PNA or ACL lectin or without any lectin, followed by FITC-avidin D. Scale bars: 50 μm. Patient 1: Becker muscular dystrophy; patient 2: limb-girdle muscular dystrophy. (**B**) Immunofluorescence images of myofiber cross-sections stained with lectins were analyzed by imaging software and normalized to that of control muscles. The data are presented as mean ± SD (n = 10–20 fibers/group). *$P < 0.05$.

that was detected even upon treatment with a very low concentration of sialidase (50 mU; Fig. 5B).

DISCUSSION

In this study, we demonstrated that the cell surface content of sialic acids was markedly reduced (by 60–80%) in skeletal muscles from dystrophic model animals—J2N-k hamsters, *mdx* mice, and *dy/dy* mice—and from patients with muscular dystrophy. By contrast, the amount of Galβ1,3GalNAc stained with ACL was not altered in dystrophic muscles. Glycosylation status has a critical pathologic significance in the genesis of dystrophy. For example, several types of dystrophic muscles show aberrant glycosylation of α-DG, which is a key molecule linking the sarcolemma to the extracellular matrix.[23] Therefore, the reduced sialic acid levels observed in this study may contribute to the severity of muscle damage in various subtypes of muscular dystrophy. A recent study reported that transgenic overexpression of a specific type of sialyltransferase (ST3Gal-II), which could lead to extensive sialylation, resulted in development of dilated cardiomyopathy.[22] However, surface sialic acid content in skeletal muscles was unexpectedly reduced because of muscle damage.[22] The pathological importance of sialic acids was suggested in distal myopathy with rimmed vacuoles,[18,20] and treatment with sialic acid metabolites prevented development of the myopathic phenotype in a mouse model.[24] Recently, sialic acids attached to ion channels through *O*-linkages were reported to modulate the gating of potassium channels[25] or the Na^+ channel NaV1.4,[26] thereby causing significant shifts in their voltage dependences. Thus, reduced sialylation in ion channel proteins may contribute to reduced muscle performance via altered action potentials in muscular dystrophy.

In a model of limb-girdle muscular dystrophy, premature senescence of satellite cells was

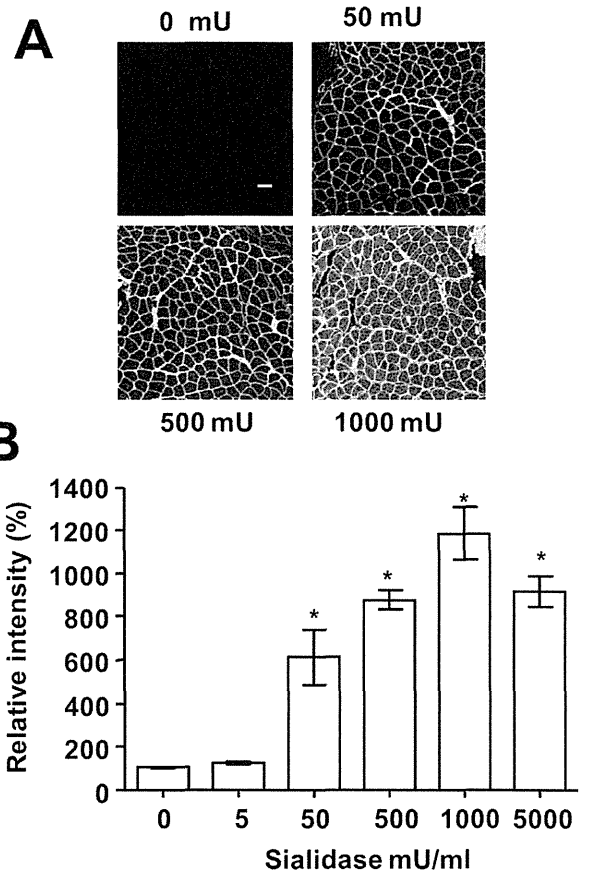

FIGURE 5. Sialidase effectively removes sialic acids and thus increases PNA staining in normal muscles. (**A**) Frozen sections of skeletal muscle from control mice were treated at 37°C for 2 h with various concentrations of sialidase and then stained with biotinylated PNA lectin, followed by FITC-avidin D. Scale bars: 50 μm. (**B**) Immunofluorescence images of myofiber cross-sections stained with PNA were analyzed by imaging software and normalized to cross-sections without sialidase treatment. The data are presented as mean ± SD (n = 50 fibers). *$P < 0.05$.

suggested to be involved in the genesis of muscular dystrophy.[27] Therefore, the aging phenomenon could be related to degeneration/regeneration cycles occurring in several myopathies. Indeed, sialic acid content has also been reported to be reduced during aging in the brain[28] and erythrocytes.[29] However, we did not observe significant differences in sialic acid content between normal skeletal muscles from 4-week-old and 6-month-old mice, and loss of sialic acid from membranes was observed whenever muscle fibers were damaged, so the reduction of sialic acid in dystrophic muscle is not likely to be due to muscle aging.

We observed that a low concentration (0.05 U/ml) of exogenously added sialidase is sufficient to remove sialic acid moieties from muscle sections of healthy mice (Fig. 5). Furthermore, PNA staining was observed in all types of muscle fibers, including necrotic, regenerating, and normally growing fibers (Fig. 3). In addition, we easily detected enhanced PNA staining in mechanically and chemically injured muscles, but not in contralateral muscles separated from injured muscles (Y. Iwata, unpublished data). Therefore, it is likely that a trace amount of sialidase is released from damaged muscle fibers, thereby cleaving surface sialic acids on and near their fibers. In contrast to low-dose sialidase (0.05 U/ml), which is sufficient for detecting changes in surface sialic acid content, we typically detect nearly 100-fold enzyme units of released CK (approximately 5 U/ml) in the serum of *mdx* mice or J2N-k hamsters.[30] Reductions in sialic acid content were also observed in the *dy/dy* mice, where CK release was not detected, despite the evident symptoms of muscle damage. Therefore, whereas surface sialic acids reduction is easily detected *in vitro*, even when only a small amount of sialidase is released from damaged muscle fibers, CK is reliably detected only when a relatively large quantity of CK is released from muscle fibers.

In addition to the accelerated release of sialidase, reduced biosynthesis of sialic acids and inhibition of sialyltransferase activity may also contribute to reduced levels of surface sialic acids. It has been reported that sialic acid concentrations *in vivo* were normal in erythrocyte membranes of patients with limb-girdle muscular dystrophy,[31] suggesting that the biosynthesis pathway of sialic acids and sialyltransferase activity were not dramatically affected by this type of muscular dystrophy. However, another study reported decreased sialyltransferase activity in the hearts of cardiomyopathic hamsters.[32]

In this study, we did not analyze in detail whether the sarcolemmal sialic acid contents are changed in heart muscles with cardiomyopathy or heart failure. However, our preliminary experiments have suggested that, similar to skeletal muscle fibers, cardiac muscles from symptomatic 11-week-old J2N-k hamsters also showed increased PNA staining compared with their healthy counterparts (Y. Iwata et al., unpublished data). Thus, sialic acid reduction may also be a marker of cell damage in cardiac and skeletal muscles, although further studies are required for generalizing the hypothesis of reduced sialic acid content to other animal models or patients with heart failure. There is a long-lasting debate concerning the involvement of stem cells in heart regeneration.[33] Given that such regenerating cells are expected to preserve surface sialic acids, positive staining of sialic acids may be useful as a method for identification of such cells.

In conclusion, we have observed that levels of sarcolemmal sialic acids were markedly reduced in dystrophic muscles, presumably via the release of cytosolic sialidase from damaged muscle fibers. Surface sialic acids are useful markers and novel therapeutic targets for damaged muscle. This highly sensitive and potentially versatile procedure may be useful for diagnostic purposes in humans, as well as for the detection of muscle damage in animal models.

The authors thank H. Ohtake for the technical assistance, and Dr. K. Komamura for kindly providing the human samples. This work was supported by a grant-in-aid for priority areas (18077015 to S.W.); grants-in-aid (23390046 to S.W., 20590874 and 23591095 to Y.I.) from the Japanese Ministry of Education, Culture, Sports, Science and Technology; and a Grant-in-Aid for Nervous and Mental Disorders (22-5 to Y.I.) from the Japanese Ministry of Health, Labour and Welfare.

REFERENCES

1. Manzur AY, Muntoni F. Diagnosis and new treatments in muscular dystrophies. Postgrad Med J 2009;85:622–630.
2. Ervasti JM, Kahl SD, Campbell KP. Purification of dystrophin from skeletal muscle. J Biol Chem 1991;266:9161–9165.
3. Campbell KP, Kahl SD. Association of dystrophin and an integral membrane glycoprotein. Nature 1989;338:259–262.
4. Ebashi S, Toyokura Y, Momoi H, Sugita H. High creatine phosphokinase activity of sera of progressive muscular dystrophy. J Biochem (Tokyo) 1959;46:103–104.
5. Vassella F, Richterich R, Rossi E. The diagnostic value of serum creatine kinase in neuromuscular and muscular disease. Pediatrics 1965; 35:322–330.
6. Nicholson GA, Morgan GJ, Meerkin M, Strauss ER, McLeod JG. The effect of aerobic exercise on serum creatine kinase activities. Muscle Nerve 1986;9:820–824.
7. Florence JM, Fox PT, Planer GJ, Brooke MH. Activity, creatine kinase, and myoglobin in Duchenne muscular dystrophy: a clue to etiology? Neurology 1985;35:758–761.
8. Straub V, Rafael JA, Chamberlain JS, Campbell KP. Animal models for muscular dystrophy show different patterns of sarcolemmal disruption. J Cell Biol 1997;139:375–385.
9. Kanagawa M, Nishimoto A, Chiyonobu T, Takeda S, Miyagoe-Suzuki Y, Wang F, et al. Residual laminin-binding activity and enhanced dystroglycan glycosylation by LARGE in novel model mice to dystroglycanopathy. Hum Mol Genet 2009;18:621–631.
10. Montanaro F, Carbonetto S. Targeting dystroglycan in the brain. Neuron 2003;37:193–196.
11. Chiba A, Matsumura K, Yamada H, Inazu T, Shimizu T, Kusunoki S, et al. Structures of sialylated O-linked oligosaccharides of bovine peripheral nerve alpha-dystroglycan. The role of a novel O-mannosyl-type oligosaccharide in the binding of alpha-dystroglycan with laminin. J Biol Chem 1997;272:2156–2162.

12. Grewal PK, Hewitt JE. Glycosylation defects: a new mechanism for muscular dystrophy? Hum Mol Genet 2003;12(spec no 2):R259–264.
13. Endo T. Dystroglycan glycosylation and its role in alpha-dystroglycanopathies. Acta Myol 2007;26:165–170.
14. Varki NM, Varki A. Diversity in cell surface sialic acid presentations: implications for biology and disease. Lab Invest 2007;87:851–857.
15. Schauer R. Achievements and challenges of sialic acid research. Glycoconj J 2000;17:485–499.
16. Schwarzkopf M, Knobeloch KP, Rohde E, Hinderlich S, Wiechens N, Lucka L, et al. Sialylation is essential for early development in mice. Proc Natl Acad Sci USA 2002;99:5267–5270.
17. Dairaku K, Miyagi T, Wakui A, Tsuiki S. Cytosolic sialidases of rat tissues with special reference to skeletal muscle enzyme. Biochem Int 1986;13:741–748.
18. Tajima Y, Uyama E, Go S, Sato C, Tao N, Kotani M, et al. Distal myopathy with rimmed vacuoles: impaired O-glycan formation in muscular glycoproteins. Am J Pathol 2005;166:1121–1130.
19. Eisenberg I, Avidan N, Potikha T, Hochner H, Chen M, Olender T, et al. The UDP-N-acetylglucosamine 2-epimerase/N-acetylmannosamine kinase gene is mutated in recessive hereditary inclusion body myopathy. Nat Genet 2001;29:83–87.
20. Noguchi S, Keira Y, Murayama K, Ogawa M, Fujita M, Kawahara G, et al. Reduction of UDP-N-acetylglucosamine 2-epimerase/N-acetylmannosamine kinase activity and sialylation in distal myopathy with rimmed vacuoles. J Biol Chem 2004;279:11402–11407.
21. Iwata Y, Katanosaka Y, Arai Y, Komamura K, Miyatake K, Shigekawa M. A novel mechanism of myocyte degeneration involving the Ca^{2+}-permeable growth factor-regulated channel. J Cell Biol 2003;161:957–967.
22. Suzuki O, Kanai T, Nishikawa T, Yamamoto Y, Noguchi A, Takimoto K, et al. Adult onset cardiac dilatation in a transgenic mouse line with Galβ1,3GalNAc α2,3-sialyltransferase II (ST3Gal-II) transgenes: a new model for dilated cardiomyopathy. Proc Jpn Acad Ser B 2011;87:550–562.
23. Ervasti JM, Campbell KP. Dystrophin and the membrane skeleton. Curr Opin Cell Biol 1993;5:82–87.
24. Malicdan MC, Noguchi S, Hayashi YK, Nonaka I, Nishino I. Prophylactic treatment with sialic acid metabolites precludes the development of the myopathic phenotype in the DMRV-hIBM mouse model. Nat Med 2009;15:690–695.
25. Schwetz TA, Norring SA, Ednie AR, Bennett ES. Sialic acids attached to O-glycans modulate voltage-gated potassium channel gating. J Biol Chem 286:4123–4132.
26. Ahrens J, Foadi N, Eberhardt A, Haeseler G, Dengler R, Leffler A, et al. Defective polysialylation and sialylation induce opposite effects on gating of the skeletal Na^+ channel NaV1.4 in Chinese hamster ovary cells. Pharmacology 87:311–317.
27. Kudryashova E, Kramerova I, Spencer MJ. Satellite cell senescence underlies myopathy in a mouse model of limb-girdle muscular dystrophy 2H. J Clin Invest 122:1764–1776.
28. Sato Y, Endo T. Alteration of brain glycoproteins during aging. Geriatr Gerontol Int 2010;10(suppl 1):S32–40.
29. Hadengue AL, Del-Pino M, Simon A, Levenson J. Erythrocyte disaggregation shear stress, sialic acid, and cell aging in humans. Hypertension 1998;32:324–330.
30. Iwata Y, Katanosaka Y, Shijun Z, Kobayashi Y, Hanada H, Shigekawa M, et al. Protective effects of Ca^{2+} handling drugs against abnormal Ca^{2+} homeostasis and cell damage in myopathic skeletal muscle cells. Biochem Pharmacol 2005;70:740–751.
31. Stibler H, Sydow O. Carbohydrate composition of erythrocyte membranes and glycosidase activities in serum in patients with myotonic dystrophy, limb-girdle dystrophy and congenital myotonia. J Neurol Sci 1984;63:285–298.
32. Bailey LE. Orotic acid prevents changes in cardiac sarcolemmal glycoproteins and contractility associated with muscular dystrophy in hamsters. Experientia 1980;36:94–95.
33. Laflamme MA, Murry CE. Heart regeneration. Nature 2011;473:326–335.

Anti-inflammatory role of PGD_2 in acute lung inflammation and therapeutic application of its signal enhancement

Takahisa Murata[a,1], Kosuke Aritake[b], Yoshiki Tsubosaka[a], Toshihiko Maruyama[b], Takayuki Nakagawa[c], Masatoshi Hori[a], Hiroyuki Hirai[d], Masataka Nakamura[e], Shuh Narumiya[f], Yoshihiro Urade[b], and Hiroshi Ozaki[a]

[a]Department of Veterinary Pharmacology, Graduate School of Agriculture and Life Sciences, University of Tokyo, Tokyo 113-8657, Japan; [b]Department of Molecular Behavioral Biology, Osaka Bioscience Institute, Osaka 565-0874, Japan; [c]Department of Veterinary Surgery, Graduate School of Agriculture and Life Sciences, University of Tokyo, Tokyo 113-8657, Japan; [d]Advanced Medicine and Development, BML, Inc., Saitama 350-1101, Japan; [e]Human Gene Sciences Center, Tokyo Medical and Dental University, Tokyo 113-8150, Japan; and [f]Department of Pharmacology, Faculty of Medicine, Kyoto University, Kyoto 606-8315, Japan

Edited by Charles N. Serhan, Brigham and Women's Hospital, Harvard Medical School, Boston, MA, and accepted by the Editorial Board February 15, 2013 (received for review October 17, 2012)

We investigated the role of prostaglandin D_2 (PGD_2) signaling in acute lung injury (ALI), focusing on its producer–effector interaction in vivo. Administration of endotoxin increased edema and neutrophil infiltration in the WT mouse lung. Gene disruption of hematopoietic PGD synthase (H-PGDS) aggravated all of the symptoms. Experiments involving bone marrow transplantation between WT and H-PGDS–deficient mice showed that PGD_2 derived from alveolar nonhematopoietic lineage cells (i.e., endothelial cells and epithelial cells) promotes vascular barrier function during the early phase (day 1), whereas neutrophil-derived PGD_2 attenuates its own infiltration and cytokine expression during the later phase (day 3) of ALI. Treatment with either an agonist to the PGD_2 receptor, DP, or a degradation product of PGD_2, 15-deoxy-$\Delta^{12,14}$-PGJ_2, exerted a therapeutic action against ALI. Data obtained from bone marrow transplantation between WT and DP-deficient mice suggest that the DP signal in alveolar endothelial cells is crucial for the anti-inflammatory reactions of PGD_2. In vitro, DP agonism directly enhanced endothelial barrier formation, and 15-deoxy-$\Delta^{12,14}$-PGJ_2 attenuated both neutrophil migration and cytokine expression. These observations indicate that the PGD_2 signaling between alveolar endothelial/epithelial cells and infiltrating neutrophils provides anti-inflammatory effects in ALI, and suggest the therapeutic potential of these signaling enhancements.

vascular permeability | pneumonia | lipid mediator | respiratory infection

Acute lung injury (ALI) and its severe manifestation, acute respiratory distress syndrome (ARDS), represent a clinical syndrome that results from multiple causes, including microbial infection and toxic inhalation. The most characteristic pathological findings of ALI/ARDS are neutrophil accumulation and alveolar edema caused by endothelial/epithelial barrier disruption (1). No specific pharmacologic therapies are currently available, and the mortality rate for ALI/ARDS remains very high (1). Thus, there is an urgent need to elucidate in detail the underlying pathogenesis of ALI/ARDS to develop new drugs against it.

Cyclooxygenase (COX), particularly COX-2 and its metabolites, the prostaglandins (PGs), play critical roles in the inflammatory response. Elevated PG levels have been reported in bronchoalveolar lavage (BAL) fluid obtained from patients with ARDS (2). In experimental models, Hinshaw et al. (3) originally found that COX inhibition prevents the development of sepsis and improves survival rates in dogs. Another group reported that COX-2 inhibition attenuated carrageenan-induced rat ALI (4). These findings suggest that COX-mediated production of PGs is crucial for the initiation and progression of lung inflammation. However, in a clinical study, treatment with the nonselective COX inhibitor ibuprofen did not reduce the incidence of ARDS in patients with sepsis (5). These observations suggest that PGs play a multifaceted role in the pathophysiology of airway inflammation, with both proinflammatory and anti-inflammatory components. The bioactions of each class of PGs are influenced by multiple causes. Types of PG-producing cells and their effector cells vary with both the causative pathogen and the stage of disease. The overall response of effector cells is determined by both receptors and cellular events. Thus, determining the precise contribution by an individual class of PGs regarding the functional partnership of its producer and effector cells at each disease stage is indispensable for future management of ALI/ARDS.

PGD_2 is one of the COX metabolites reported to mediate an inflammatory response (6). The hematopoietic-type PGD_2 synthase (H-PGDS) is expressed mainly in hematopoietic lineage cells, such as mast cells and Th2 cells. PGD_2 displays its bioactivity through the G protein-coupled receptor DP and/or the chemoattractant receptor-homologous molecule expressed on Th2 cells (CRTH2). Several previous studies have demonstrated that DP signal activation inhibits the migration and/or activation of eosinophils, basophils, dendritic cells, and Th2 cells (6). On the other hand, CRTH2 signal activation results in the migration of eosinophils and Th2 cells (7, 8). The dehydration product of PGD_2, 15-deoxy-$\Delta^{12,14}$-PGJ_2 (15d-PGJ_2), also modulates inflammatory responses via peroxisome proliferator-activated receptor (PPAR)-γ–dependent or –independent signal activation (9). Like the other PGs, PGD_2 presumably changes its pathophysiological contribution through these signal pathways depending on the target tissue, type of stimulus, and stage of the disease.

In a previous study, we focused on the physiological function of PGD_2-DP signaling in neovascular endothelial cells of tumors, and found that stimulation of this pathway enhanced endothelial barrier function and suppressed tumor angiogenesis (10). Given that vascular endothelial cells and alveolar epithelial cells form their respective barriers in the lung, which is a crucial determinant of lung inflammation, these observations led us to hypothesize that PGD_2 might play a protective role in ALI/ARDS. Consequently, in the present study we attempted to explore the pathophysiological implications of PGD_2 biosynthesis in the development ALI/ARDS

Author contributions: T. Murata and Y.U. designed research; T. Murata, K.A., Y.T., and T. Maruyama performed research; T. Murata, K.A., T.N., M.H., H.H., M.N., S.N., Y.U., and H.O. contributed new reagents/analytic tools; T. Murata, K.A., Y.T., and T. Maruyama analyzed data; and T. Murata wrote the paper.

The authors declare no conflict of interest.

This article is a PNAS Direct Submission. C.N.S. is a guest editor invited by the Editorial Board.

[1]To whom correspondence should be addressed. E-mail: amurata@mail.ecc.u-tokyo.ac.jp.

This article contains supporting information online at www.pnas.org/lookup/suppl/doi:10.1073/pnas.1218091110/-/DCSupplemental.

by focusing on the interaction between alveolar endothelial/epithelial cells and infiltrating neutrophils.

Results

Host H-PGDS Deficiency Accelerates Lung Inflammation. Under normal conditions, H-PGDS–deficient (H-PGDS$^{-/-}$) mice did not display any functional defect in respiratory gas exchange, as quantified by arterial partial pressure of oxygen (pO_2) values (Fig. 1*A*). Intratracheal administration of lipopolysaccharide (LPS), 3.75 mg/kg for 3 d, impaired respiratory function in both WT and H-PGDS$^{-/-}$ mice. Compared with the WT mice, the H-PGDS$^{-/-}$ mice exhibited more severe lung damage and a lower survival rate (Fig. 1*B*).

Morphological studies showed that the LPS challenge induced neutrophil infiltration in the lungs of WT mice by day 3 (Fig. 1*C*). The H-PGDS$^{-/-}$ mice exhibited more severe damage. The LPS challenge increased both the protein content of BAL fluid and the myeroperoxidase (MPO) activity of lung homogenate, an indicator of neutrophil infiltration (Fig. 1 *D* and *E*). These injury severity scores peaked by day 3 and normalized by day 10 (MPO score on day 10 WT, 42 ± 5 U/mg; H-PGDS$^{-/-}$, 64 ± 12 U/mg; n = 4 each). Both BAL protein content and MPO activity were higher in H-PGDS$^{-/-}$ mice compared with WT mice throughout the test period.

LPS inhalation increased PGD_2 production in the lungs of WT mice, peaking on day 1 (Fig. 1*F*). However, little PGD_2 production was detected in the lungs of H-PGDS$^{-/-}$ mice, suggesting that H-PGDS is a principal source of PGD_2 in this model. The foregoing observations indicate that PGD_2 is an anti-inflammatory mediator in endotoxin-induced ALI.

H-PGDS Deficiency Accelerates Fluid Accumulation, Vascular Permeability, and Cytokine Expression in Inflamed Lung. An LPS challenge induces inflammatory mediators that inhibit barrier formation of alveolar endothelial/epithelial cells. Without LPS inhalation, there was no difference between the WT and H-PGDS$^{-/-}$ mice (Fig. 2*A*). LPS inhalation slightly, but not significantly, increased the lung water content in the WT mice but caused obvious edema in the H-PGDS$^{-/-}$ mice. Dye extravasation was monitored to evaluate whether PGD_2 production can directly and acutely influence alveolar vascular permeability. In both lines of mice, the LPS challenge increased lung vascular leakage (Fig. 2 *B* and *C*). In H-PGDS$^{-/-}$ mice, much more dye was extravasated, suggesting the importance of PGD_2 in protecting the alveolar vascular barrier.

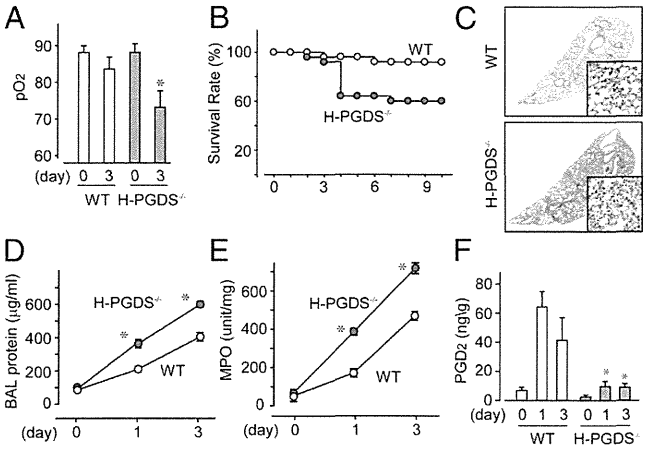

Fig. 1. H-PGDS deficiency worsens endotoxin-induced lung inflammation. (*A* and *B*) Arterial pO_2 (*A*; n = 5 each) and survival rate (*B*; n = 30 each) were monitored. (*C*) Lung morphology was examined (n = 6–8). (Scale bar: 100 μm.) (*D*) BAL fluid was collected, and protein content was measured (n = 8–9). (*E* and *F*) MPO activity (*E*) and PGD_2 content (*F*) in lung tissue homogenates were measured (*E*, n = 8 each; *F*, n = 4–5). Results are presented as the ratio of tissue dry and wet weights. *P < 0.05 compared with WT.

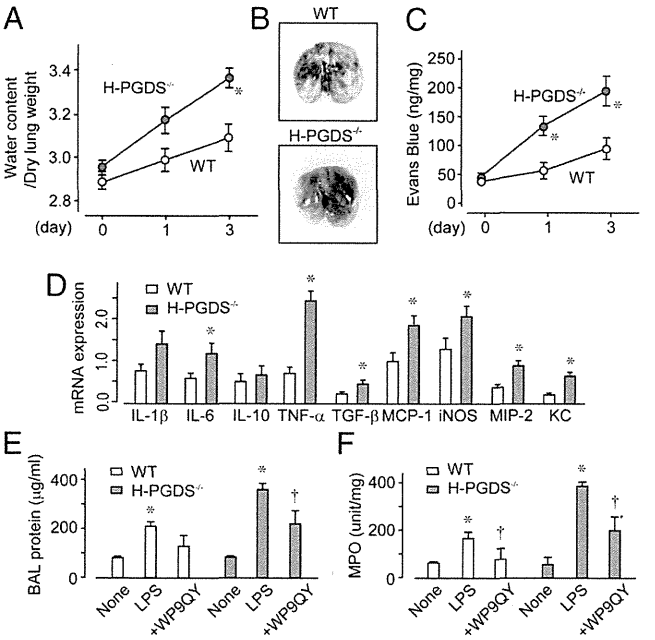

Fig. 2. H-PGDS deficiency disrupts the vascular barrier and accelerates cytokine expression in an inflamed lung. (*A*) Lung water content was calculated (n = 10–12). (*B*) On day 3, Evans blue dye was injected i.v. and circulated for 30 min. (*C*) Dye content of the lung, shown as the ratio to tissue dry weight (n = 8–10). (*D*) mRNA expression of each cytokine in LPS-treated lungs on day 1, shown as the ratio of GAPDH (n = 5 each). *P < 0.05 compared with WT. (*E* and *F*) TNF-α inhibitory peptide WP9QY was administered to the LPS-challenged mice, and the protein content in BAL fluid (*E*) and MPO activity (*F*) were measured on day 1 (n = 6 each). *,†P < 0.05 compared with nontreated and LPS-treated mice.

Quantitative RT-PCR demonstrated that the LPS challenge elevated the mRNA expression of multiple proinflammatory cytokines in the lungs of WT mice on day 1 (Fig. 2*D*). Host H-PGDS deficiency further exacerbated these results. Of particular note, TNF-α expression was elevated almost 3.3-fold in H-PGDS$^{-/-}$ mice. We previously reported that H-PGDS deficiency resulted in elevated TNF-α production, which in turn further stimulated inflammation in a tumor microenvironment (11). As expected with these observations, intranasal treatment with the TNF-α inhibitory peptide WP9QY (10 mg/kg) inhibited the inflammatory response in the H-PGDS$^{-/-}$ mice (Fig. 2 *E* and *F* and Fig. S1*A*). The enhanced inflammatory responses seen in H-PGDS$^{-/-}$ mice can be attributed, at least in part, to the increased TNF-α production.

Contribution of Hematopoietic Cell-Derived PGD_2 in Lung Inflammation. Immunostaining revealed that infiltrating Gr-1–positive neutrophils strongly expressed H-PGDS in inflamed WT mouse lung on day 3 (Fig. 3*A*, *Upper*). Platelet endothelial cell adhesion molecule (PECAM)-1–positive endothelial cells and E-cadherin–positive epithelial cells also expressed H-PGDS (Fig. 3 *B* and *C*), but at relatively low levels. No signal was detectable by anti–H-PGDS antibody in inflamed H-PGDS$^{-/-}$ lung (Fig. 3*A*, *Lower*).

Because PGD_2-mediated signaling appeared to be activated in both endothelial/epithelial cells and neutrophils, we next investigated the contributions of these two PGD_2 sources to the progression of ALI. Transplantation of H-PGDS$^{-/-}$ bone marrow (BM) exacerbated ALI, particularly in the later phase (day 3), in WT mice (compare WT+H-PGDS$^{-/-BM}$ and WT+WT^{BM}; Fig. 3*D*). Conversely, transplantation of WT^{BM} diminished later-

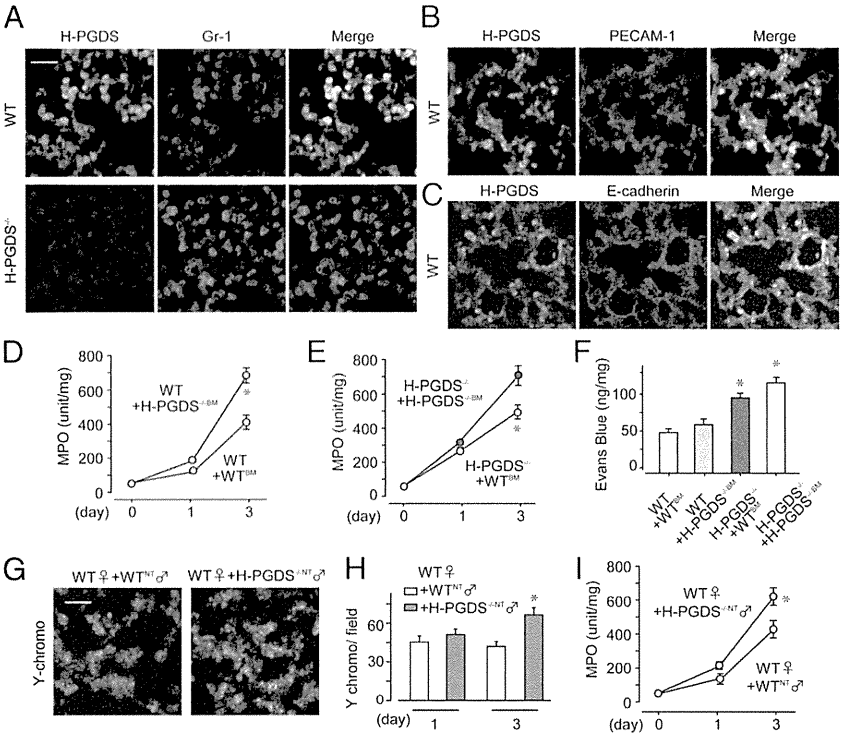

Fig. 3. Alveolar nonhematopoietic cell-derived PGD_2 contributes to form a barrier in early-phase ALI, and leukocyte-derived PGD_2 autocrinely inhibits infiltration in later-phase ALI. (*A–C*) H-PGDS expression was detected in neutrophils (*A*), endothelial cells (*B*), and epithelial cells (*C*) on day 3 ($n = 5–6$ each). (Scale bar: 50 μm.) (*D* and *E*) After bone marrow transplantation, MPO activity was measured in WT (*D*) and H-PGDS$^{-/-}$ (*E*) mice ($n = 8$ each). (*F*) Dye extravasation was monitored on day 1 ($n = 8–10$). (*G–I*) Female WT mice injected with male mouse-origin H-PGDS$^{-/-}$ or WT neutrophils were subjected to LPS inhalation. (*G*) Y chromosomes were labeled in lung sections on day 3. (Scale bar: 50 μm.) (*H*) Number of Y chromosome-positive neutrophils in fields ($n = 8$ each). (*I*) MPO activity ($n = 8$ each). *$P < 0.05$ compared with WT +WT^{BM} (*D* and *F*), H-PGDS$^{-/-}$ +H-PGDS$^{-/-BM}$ (*E*), or WT+WT^{NT} (*H* and *I*).

phase ALI in H-PGDS$^{-/-}$ mice (compare H-PGDS$^{-/-}$+WT^{BM} and H-PGDS$^{-/-}$+H-PGDS$^{-/-BM}$; Fig. 3*E*). These findings demonstrate the importance of BM-derived hematopoietic cells, mostly neutrophils, as a functional source of PGD_2 at the progression stage of ALI. At an early phase of ALI (day 1), H-PGDS deficiency in mice of nonhematopoietic lineage (H-PGDS$^{-/-}$+WT^{BM}/H-PGDS$^{-/-}$+H-PGDS$^{-/-BM}$; Fig. 3 *D* and *E*) was associated with increased ALI scores regardless of the genotype of hematopoietic lineage cells (compare with WT+H-PGDS$^{-/-BM}$/WT+WT^{BM}). These observations show the functional impact of PGD_2 produced by nonhematopoietic alveolar cells (i.e., endothelial cells and epithelial cells) at the initiation of ALI.

We next investigated how PGD_2 derived from hematopoietic cells and PGD_2 derived from nonhematopoietic cells affect vascular barrier formation in the lung. Hematopoietic lineage-specific H-PGDS deficiency (WT+H-PGDS$^{-/-BM}$) did not substantially affect vascular permeability on day 1 (compare with WT+WT^{BM}; Fig. 3*F*), but nonhematopoietic lineage-specific H-PGDS deficiency (H-PGDS$^{-/-}$+WT^{BM}) disrupted the vascular barrier. This result suggests that PGD_2 production in cells of nonhematopoietic origin is crucial for protection of the vascular barrier in the current model of ALI.

We performed a neutrophil invasion assay to evaluate the importance of neutrophils in PGD_2-mediated immunosuppression. Neutrophils isolated from male H-PGDS$^{-/-}$ mice (H-PGDDS$^{-/-NT}$) or WT mice (WT^{NT}) were injected additively into female WT mice subjected to LPS inhalation, and infiltration of Y chromosome-positive neutrophils was assessed. During the early phases of ALI, no differences in either invasiveness (Fig. 3*H*) or MPO score (Fig. 3*I*) were detected in the two groups of mice; however, in a later phase of ALI, the H-PGDS$^{-/-NT}$ mice demonstrated a greater degree of invasiveness (Fig. 3 *G* and *H*) and thus elevated MPO scores (Fig. 3*I*). At this later phase, neutrophil-derived PGD_2 is presumed to suppress cell invasiveness following an autocrine signaling mechanism.

Roles of the PGD_2-DP and PGD_2-PGJ_2 Axes in ALI. We next investigated the involvement of each PGD receptor in PGD_2-mediated ALI suppression. In response to LPS inhalation, the lungs of DP-deficient (DP$^{-/-}$) mice, but not those of CRTH2-deficient (CRTH2$^{-/-}$) mice, demonstrated less efficient gas exchange (Fig. 4*A*), resulting in a lower survival rate (Fig. 4*B*). The lungs of DP$^{-/-}$ mice consistently showed both elevated MPO scores (Fig. 4*C*) and severe histological damage (Fig. 4*D*); however, these symptoms were still not as severe as those seen in the H-PGDS$^{-/-}$ mice (MPO score on day 3: DP$^{-/-}$, 592 ± 11; H-PGDS$^{-/-}$, 734 ± 23). This result implies a role for signal pathways other than the PGD_2-DP receptor axis in PGD_2-mediated immunosuppression.

We then investigated whether PGD_2-signal enhancement can protect against lung inflammation. In LPS-treated WT and H-PGDS$^{-/-}$ mice, intranasal administration of a DP receptor agonist, BW245C, or a degraded product of PGD_2, 15d-PGJ_2 (both at 100 μg/kg), enhanced the survival rate (Fig. 4*E*) and lowered the MPO score (Fig. 4*F*). Administration of a CRTH2 agonist DK-PGD_2 did not produce the same improvements, however.

Given that bacterial sepsis is one of the most common causes of ALI, numerous investigators have used the administration of endotoxin to initiate ALI. LPS-induced inflammatory changes are relatively mild and transient, however. In another standard model, oleic acid (OA) is used to induce ALI, which produces significantly more severe histopathological changes, similar to those observed in ARDS. In the present study, administration of OA (150 μL/kg) in addition to LPS (1.5 mg/kg) caused very severe alveolar damage. At 2 h after OA administration to WT mice, damage to the lung was characterized by extensive neutrophil infiltration, pulmonary hemorrhage (Fig. S1 *B* and *C*), respiratory dysfunction (Fig. 4*G*), and alveolar edema (Fig. 4*H*). Preadministration of either BW245C or 15d-PGJ_2 effectively diminished the injuries seen in this severe ALI/ARDS model, suggesting these agents' strong potential for therapeutic application.

Immunostaining of LPS-challenged WT mouse lung (on day 3) revealed DP-positive signals in both Gr-1–positive neutrophils (Fig. 5*A*) and PECAM-1–positive endothelial cells (Fig.

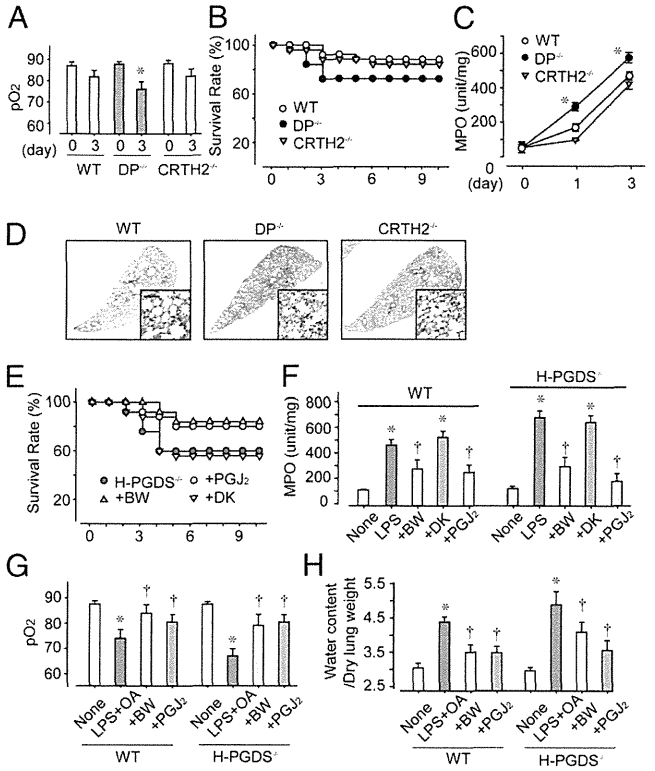

Fig. 4. (*A–D*) PGD_2-DP and PGD_2-PGJ_2 axes contribute to ALI suppression. LPS was administered to WT, $DP^{-/-}$, and $CRTH2^{-/-}$ mice, and pO_2 (*A*; $n = 5$ each), survival rate (*B*; $n = 30$ each), and MPO activity (C; $n = 8–10$ each) were monitored. (*D*) H&E staining on day 3. (Scale bar: 100 μm.) $^*P < 0.05$ compared with WT. (*E–H*) DP agonism or PGJ_2 signal enhancement is beneficial against ALI/ARDS. BW245C or 15d-PGJ_2 was administered to LPS-challenged mice and LPS+OA-challenged mice. Survival rate (*E*; $n = 25–30$) and MPO activity (*F*; $n = 8–10$) were monitored in LPS-challenged mice, and pO_2 (*G*; $n = 5$ each) and lung tissue water (*H*; $n = 8–10$) levels were monitored in LPS+OA-challenged mice at 2 h after the challenge. $^{*,\dagger}P < 0.05$ compared with LPS/LPS+OA-treated and nontreated mice.

5*B*), but not in E-cadherin–positive epithelial cells (Fig. 5*C*). These findings verify the functional contribution of DP receptors in ALI. Hematopoietic lineage-specific DP deficiency did not influence neutrophil infiltration in the WT lung (Fig. 5*D*; compared $WT+WT^{BM}$ and $WT+DP^{-/-BM}$). $DP^{-/-}+DP^{-/-BM}$ mice had significantly higher MPO scores than $WT+WT^{BM}$ mice throughout the test period. Interestingly, hematopoietic reconstitution using WT mice ($DP^{-/-}+WT^{BM}$) did not change the severity of inflammation in $DP^{-/-}$ mice (Fig. 5*E*). These findings suggest the importance of the DP-mediated signals in nonhematopoietic alveolar cells, presumably endothelial cells, in anti-inflammatory effects during ALI. In line with this idea, DP agonism was not seen in mice with a nonhematopoietic lineage-specific DP deficiency ($DP^{-/-}+WT^{BM}$) on day 3 (Fig. 5*F*). Treatment with 15d-PGJ_2 was effective regardless of the hematopoietic genotype.

We next examined the impact of DP-mediated signals on vascular barrier formation and neutrophil motility. On a dye extravasation assay, mice lacking DP from a nonhematopoietic lineage ($DP^{-/-}+WT^{BM}$ and $DP^{-/-}+DP^{-/-BM}$) exhibited defective vascular barrier formation on day 3 regardless of hematopoietic genotype (Fig. 5*G*). As demonstrated by the neutrophil infiltration assay, DP deficiency in the neutrophils of LPS-challenged WT mice did not affect the infiltrative capability of these cells on day 3 (Fig. 5*H*). This finding reinforces the crucial role of the PGD_2-DP signal axis in nonhematopoietic alveolar cells in protecting the vascular barrier against inflammation.

DP Agonist, But Not PGJ_2, Inhibits Vascular Permeability in Vitro. ALI progression has three main phases: cytokine expression, vascular barrier disruption, and neutrophil infiltration. In vitro LPS treatment (50 ng/mL for 6 h) of both WT and H-$PGDS^{-/-}$ mouse lung endothelial cells (MLECs) resulted in elevated mRNA expression of TNF-α (Fig. 6*A*). In line with the in vivo data, H-$PGDS^{-/-}$ MLECs were more responsive to LPS challenge compared with WT MLECs. Pretreatment with DP agonist BW245C (0.3 μM) or 15d-PGJ_2 (0.3 μM) attenuated the elevated gene expression of TNF-α in both MLEC lines.

Treatment with PGD_2 (1–3 μM) or the DP agonist BW245C (0.1–0.3 μM) increased transendothelial electrical resistance (TER), indicating decreased permeability in human pulmonary arterial endothelial cells (Fig. 6 *B* and *C*). Consistent with our previous study showing that DP agonism tightens the endothelial barrier through cAMP–protein kinase A activation in bovine aortic endothelial cells (10), treatment with the cAMP booster forskolin (1 μM) enhanced endothelial barrier formation. In contrast, treatment with the CRTH2 agonist DK-PGD_2 (0.3–1 μM) or 15d-PGJ_2 (0.3–1 μM) did not affect endothelial barrier formation in vitro.

In the transmembrane migration assay, isolated neutrophils migrated toward a solution of 10 nM leukotriene B_4 (LTB_4) added to the lower chamber (Fig. 6*D*). The addition of 15d-PGJ_2 (1 μM) significantly inhibited LTB_4-induced neutrophil migration, with no agonism resulting from the addition of BW245C (0.3 μM) or DK-PGD_2 (1 μM).

The foregoing in vitro experiments suggest that PGD_2 plays an anti-inflammatory role in ALI through either of two different signaling pathways: DP-dependent or PGJ_2-dependent. The DP-mediated signaling is found mainly in endothelial cells, whereas PGJ_2-mediated signaling is seen in various other cell types.

Discussion

The main purpose of the present study was to define the roles of PGD_2-mediated signals in the pathogenesis of ALI, focusing on its producer–effector interaction in vivo. We have demonstrated that the functional source of PGD_2 shifts from alveolar endothelial/epithelial cells to infiltrating neutrophils along with ALI progression, and that the PGD_2 thus produced represents an anti-inflammatory response through DP-mediated signaling arising mainly in endothelial cells and PGJ_2 signaling in various other types of cells (Fig. S2).

PGs play paradoxical roles, both proinflammatory and anti-inflammatory, in injured lungs (12). Major PGs, including thromboxane A_2 (TXA_2) and PGE_2, are classified mostly as proinflammatory PGs in ALI. Treatment with TXA_2 synthase inhibitor or gene deficiency of PGE receptor EP3 has been found to attenuate lung edema in mice (13, 14). In contrast, anti-inflammatory roles for lipoxin A_4 and 15d-PGJ_2 have been reported in mouse ALI models (15, 16). Apparently, ALI induction is intricately modulated by a variety of PGs. Given that the pathophysiological action of each PG varies with its engaged receptor subtypes, target cells, and context of activation, a detailed evaluation of the role of each PG with respect to its source and effector is indispensable to unraveling this complexity and ultimately overcoming ALI.

Our observations consistently demonstrate the anti-inflammatory effects of PGD_2, as well as the related therapeutic potential of DP agonism and PGJ_2 treatment in ALI/ARDS models. Some previous studies have suggested a proinflammatory role for PGD_2 in certain respiratory disorders, with the mechanisms mediated through signaling pathways other than those that we have studied here. Monneret et al. (17) reported that PGD_2 inhalation caused bronchoconstriction by cross-reacting with the

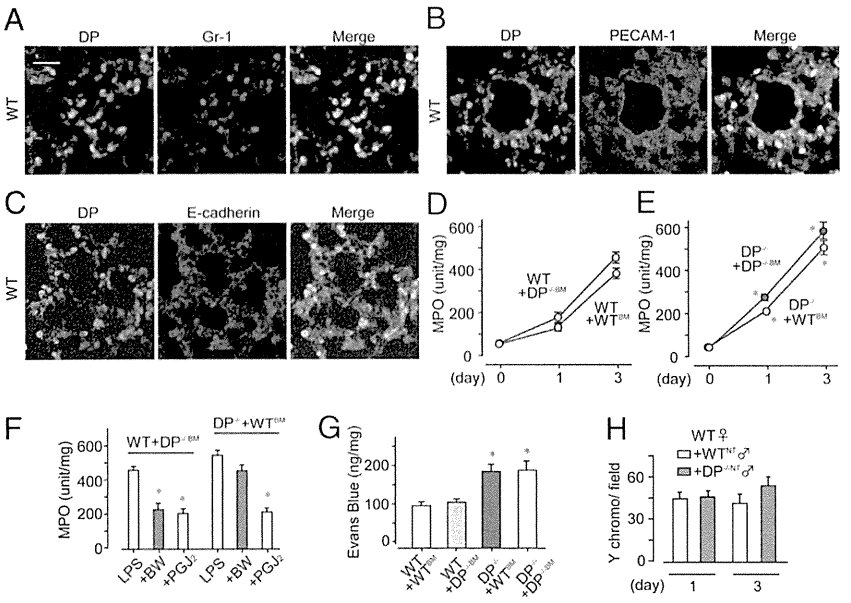

Fig. 5. DP activation in endothelial cells is beneficial against ALI. (*A–C*) DP protein expression was detected in neutrophils (*A*) and endothelial cells (*B*), but not in epithelial cells (*C*), on day 3 ($n = 5$ each). (Scale bar: 50 μm.) (*D* and *E*) After bone marrow transplantation, MPO activity was monitored in WT, $DP^{-/-}$, and $CRTH2^{+}$ mice ($n = 8$ each). (*F* and *G*) BW245C or 15d-PGJ_2 was administered to LPS-challenged mice, and MPO activity (*F*; $n = 6–8$) and dye extravasation (*G*; $n = 6–8$) were monitored on day 3. (*H*) The infiltrating ability of $DP^{-/-}$ neutrophils isolated from male mice into inflamed WT lung was monitored on day 3 ($n = 8$ each). $^{*,\dagger}P < 0.05$ compared with WT+WT^{BM} (*E*), LPS-treated (*F*), and WT+WT^{NT} (*G*) mice.

TXA_2 receptor TP. Another group reported that PGD_2 causes eosinophil and basophil chemotaxis by interacting with a CRTH2 receptor (7). Like the other PGs, PGD_2 appears to have a dual role, tissue-protective or tissue-invasive in the context of airway inflammation. This action may depend on the specific receptor involved, the specific type of pathogenesis occurring, and the severity and stage of the disease.

Clearly identifying the types of cells playing the greatest roles in the responses to these related respiratory pathologies is difficult, particularly in vivo. We found that hematopoietic replacement allowed us to determine the active histocellular site of PGD_2 signaling in the ALI model. Using this procedure, we determined that the PGD_2-DP signaling arising in lung cells of nonhematopoietic origin (i.e., endothelial/epithelial cells) is responsible for the anti-inflammatory response in early stages of ALI (Figs. 3 *D–F* and 5 *D–G*). In contrast, PGD_2 produced by hematopoietic origin, most likely neutrophils, play a central role in the immunosuppressive response in the later stages of ALI. As an effector signal, the DP-mediated anti-inflammatory response of native resident lung cells is involved in all phases of ALI. Given the strong links among vascular permeability, immune cell infiltration, and cytokine induction, determining the specific contributions of DP-mediated anti-inflammatory reactions in vivo is difficult. However, our data derived from both dye extravasation experiments (Fig. 5*G*) and in vitro experiments clearly indicate that PGD_2-DP signaling acutely and directly inhibited alveolar vascular permeability (Fig. 6 *B* and *C*). Furthermore, we found that DP-stimulation targeting mainly to endothelial cells strongly inhibited the symptoms of ALI (Fig. 5*F*). Teijaro et al. (18) recently reported that a proinflammatory cytokine burst in vascular endothelial cells is the major factor promoting infection-induced ALI. Although detailed investigations are needed to clarify the contributions of PGD_2 signaling to epithelial immune responses, the application of endothelial suppressants might be a rational strategy against ALI/ARDS.

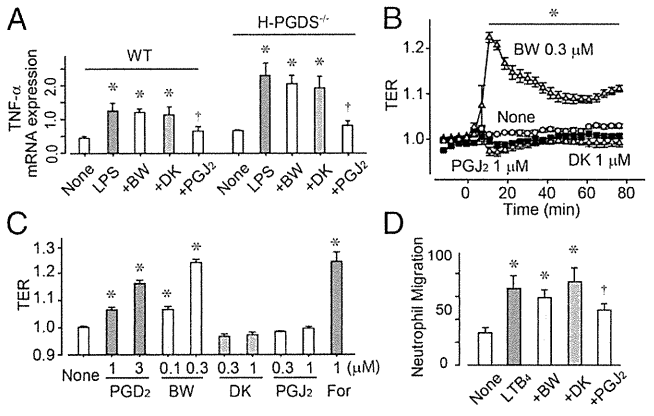

Fig. 6. PGJ_2 signal inhibits cytokine expression in endothelial cells and neutrophil migration, and DP agonism enhances endothelial barrier formation. (*A*) mRNA expression of TNF-α in mouse lung endothelial cells, shown as the ratio of GAPDH ($n = 5$ each). (*B* and *C*) TER; typical responses are shown in *B*, and data are summarized in *C* ($n = 4–6$). (*D*) Transmembrane migration assay performed using isolated neutrophils. LTB_4 was added to the lower chamber and test agents were added to both the lower and upper chambers. Data represent the number of migrating cells to lower chambers in one field (20×; $n = 5$ each). $^{*,\dagger}P < 0.05$ compared with nontreated or LPS-treated cells.

In the present study, H-PGDS deficiency enhanced the inflammatory response to a much greater degree than DP deficiency, suggesting the existence of an alternative signaling pathway in addition to the DP-mediated pathway. Lipoxins are anti-inflammatory lipid mediators that potently inhibit neutrophil infiltration (19). In preliminary experiments, we investigated the possibility that PGD_2 produces an anti-inflammatory reaction by stimulating lipoxin production, but detected no definite correlation between these two mediators (Fig. S3 *A–D*). It is also well known that a degraded product of PGD_2, 15d-PGJ_2, exerts anti-inflammatory effects through either a PPAR-γ–dependent pathway or a PPAR-γ–independent pathway. We have shown here that administration of 15d-PGJ_2 produces a therapeutic action against ALI/ARDS in vivo (Fig. 4 *E–H*). Our in vitro experiments suggest that 15d-PGJ_2–mediated suppression of both cytokine expression and neutrophil migration contribute to this action (Fig. 6 *A* and *D*). Genovese et al. (20) reported that administration of the PPAR-γ agonist rosiglitazone or 15d-PGJ_2 moderates bleomycin-induced mouse lung injury. Another group demonstrated that 15d-PGJ_2 is protective against carrageenan-induced ALI through a nuclear factor erythroid 2-related factor-2 (Nrf-2)-mediated transcriptional pathway (16). Rajakariar et al. (21) reported that 15d-PGJ_2 is produced at sufficient levels in vivo to drive the resolution of zymosan-induced mouse peritonitis.

Thus, PGD_2 may produce an anti-inflammatory effect in ALI, in part through PGJ_2-dependent signaling pathways.

In summary, PGD_2 is an anti-inflammatory mediator in endotoxin-induced ALI, and enhancing its signal can be beneficial in the treatment of ALI/ARDS. The site of PGD_2 activity shifts from native lung resident cells to infiltrating immune cells during the pathological progression of ALI.

Materials and Methods

Experimental Animals and ALI Induction. All experiments were approved by the University of Tokyo's Institutional Animal Care and Use Committee. H-PGDS$^{-/-}$, DP$^{-/-}$, and CRTH2$^{-/-}$ mice (C57BL/6) were generated and bred as described previously (22–24). For BM transplantation, 5-wk-old female mice received 9 Gy irradiation for BM ablation. BM cells (2×10^6) freshly isolated from donor mice were injected into the tail vein of the recipient. The mice were used for the experiments at 6 wk after transplantation.

To induce ALI, female mice (25 g) were anesthetized with 1.5% isoflurane, and *Escherichia coli* endotoxin LPS (O55:B5; 3.75 mg/kg) was instilled intratracheally. Intranasal administration of WP9QY (10 mg/kg), BW245C (100 μg/kg), DK-PGD_2 (100 μg/kg), or 15d-PGJ_2 (100 μg/kg) was started 10 min before the LPS challenge and then repeated every 3 h for WP9QY or every 12 h for the other agents. OA (0.15 mL/kg) was administered i.v. at 30 min after the instillation of LPS (1.5 mg/kg) to provoke severe inflammation.

Analysis of BAL Fluid, Blood Gases, and Lung Edema. BAL was collected by flushing the lung with 1 mL of saline solution although a tracheal annula. Protein concentrations in BAL were measured. For blood gas measurements, blood drawn from the abdominal aorta was analyzed with an i-STAT blood analyzer (FUSO Pharmaceutical Industries) following the manufacturer's instructions.

To measure lung water content, the excised lungs were weighed, then dried and reweighed. Water content was calculated by subtracting the dry weight from the wet weight. For permeability assessment, Evans blue dye (30 mg/kg) was injected i.v. and circulated for 3 h. Mice were killed and perfused with saline solution. Extravasated dye into lung tissue was extracted in formamide, and the contents were quantified spectrophotometrically.

PGD_2 Measurement and MPO Assay. Dissected lungs were homogenized in ethanol containing 0.02% HCl, and the samples were separated by HPLC. MS was performed using an API 3200 triple-quadruple tandem mass spectrometer (AB SCIEX). For MPO assays, dissected lungs were homogenized in potassium phosphate buffer containing 0.3% hexadecyltrimenthyl ammonium bromide. After centrifugation, supernatant was collected. Then 0.5 mM *o*-dianisidine dihydrochloride (MP Biochemicals) and 0.05% hydrogen peroxide were added to the supernatant, and optical density was measured at 460 nm.

Morphological Studies. Paraffin-embedded sections (4 μm) were used for H&E staining. Cryosections (5 μm) were used for all other stainings. Primary antibodies included anti–H-PGDS, DP (Cayman Chemicals), anti–Gr-1, anti-CD31, and anti–E-cadherin (BD Biosciences) antibodies. In some experiments, cryosections were labeled with biotin-labeled DNA probes against the Y chromosome (Chromosome Science), following the manufacturer's protocol.

Isolation of MLECs and Quantitative RT-PCR. Lung tissue was dissected, minced in 0.1% collagenase, and homogenized. Magnetic beads (Dynal) coated with anti–ICAM-2 antibodies (BD Pharmingen) were added to the cells. After a 1-h incubation, endothelial cells were collected using a magnetic holder, washed, and plated and passaged for use. After 48 h, serum-starved endothelial cells were used for experiments.

Total RNA was isolated and reverse-transcribed into cDNA. Subsequent quantitative PCR using platinum SYBR Green qPCR SuperMix-UDG (Invitrogen) and specific primers was performed with an ABI Prism 7000 (Applied Biosystems).

TER Measurement. Endothelial barrier integrity was evaluated by measuring TER using an Xcelligence real-time cell analyzer DP system (Roche). In brief, human pulmonary arterial endothelial cells were seeded on gold electrodes and incubated overnight, after which electrical resistance across the cell layer was determined. The TER value thus derived was divided by the initial value for normalization.

Isolation of Neutrophil and Chemotaxis Assay. Marrow cavities of the tibias and femurs of 8-wk-old mice were flushed with DMEM with 10% FCS. Neutrophils were isolated by centrifugation over discontinuous Percoll gradients. For neutrophil invasion assays, 5×10^6 neutrophils were injected into tail veins of recipient mice each day.

A modified Boyden chamber with 8-μm pores (BD Biosciences) was used for chemotaxis assays. Stimulants were added to the bottom chamber, and inhibitors were added to both the upper and bottom chambers. Isolated neutrophils (2×10^5 cells) were applied to the upper chambers. After 1 h, cells on the membrane were fixed and stained with Giemsa solution. The number of cells from five randomly chosen fields (200×) on the lower side of the membrane was counted.

Statistical Analyses. All data are presented as mean ± SEM. Statistical differences were determined using the Student *t* test for two-group comparisons and one-way ANOVA with Dunnett's test for multiple-group comparisons.

ACKNOWLEDGMENTS. This work was supported by a Grant-in-Aid for Young Scientists (A) and a Grant-in-Aid for Challenging Exploratory Research from the Ministry of Education, Culture, Sports, Science and Technology, and by the Japan Society for the Promotion of Science, Takeda Science Foundation, and Pharmacological Research Foundation, Tokyo.

1. Ware LB, Matthay MA (2000) The acute respiratory distress syndrome. *N Engl J Med* 342(18):1334–1349.
2. Frank JA, Matthay MA (2005) Leukotrienes in acute lung injury: A potential therapeutic target? *Am J Respir Crit Care Med* 172(3):261–262.
3. Hinshaw LB, Solomon LA, Erdös EG, Reins DA, Gunter BJ (1967) Effects of acetylsalicylic acid on the canine response to endotoxin. *J Pharmacol Exp Ther* 157(3):665–671.
4. Cuzzocrea S, et al. (2002) Protective effects of Celecoxib on lung injury and red blood cells modification induced by carrageenan in the rat. *Biochem Pharmacol* 63(4): 785–795.
5. Bernard GR, et al.; The Ibuprofen in Sepsis Study Group (1997) The effects of ibuprofen on the physiology and survival of patients with sepsis. *N Engl J Med* 336(13): 912–918.
6. Kostenis E, Ulven T (2006) Emerging roles of DP and CRTH2 in allergic inflammation. *Trends Mol Med* 12(4):148–158.
7. Hirai H, et al. (2001) Prostaglandin D_2 selectively induces chemotaxis in T helper type 2 cells, eosinophils, and basophils via seven-transmembrane receptor CRTH2. *J Exp Med* 193(2):255–261.
8. Honda K, et al. (2003) Prostaglandin D_2 reinforces Th2 type inflammatory responses of airways to low-dose antigen through bronchial expression of macrophage-derived chemokine. *J Exp Med* 198(4):533–543.
9. Scher JU, Pillinger MH (2005) 15d-PGJ_2: The anti-inflammatory prostaglandin? *Clin Immunol* 114(2):100–109.
10. Murata T, et al. (2008) Role of prostaglandin D_2 receptor DP as a suppressor of tumor hyperpermeability and angiogenesis in vivo. *Proc Natl Acad Sci USA* 105(50): 20009–20014.
11. Murata T, et al. (2011) Prostagladin D_2 is a mast cell-derived antiangiogenic factor in lung carcinoma. *Proc Natl Acad Sci USA* 108(49):19802–19807.
12. Gilroy DW, et al. (1999) Inducible cyclooxygenase may have anti-inflammatory properties. *Nat Med* 5(6):698–701.
13. Ishitsuka Y, et al. (2004) Involvement of thromboxane A_2 (TXA_2) in the early stages of oleic acid-induced lung injury and the preventive effect of ozagrel, a TXA_2 synthase inhibitor, in guinea-pigs. *J Pharm Pharmacol* 56(4):513–520.
14. Göggel R, Hoffman S, Nüsing R, Narumiya S, Uhlig S (2002) Platelet-activating factor-induced pulmonary edema is partly mediated by prostaglandin E(2), E-prostanoid 3-receptors, and potassium channels. *Am J Respir Crit Care Med* 166(5):657–662.
15. Fukunaga K, Kohli P, Bonnans C, Fredenburgh LE, Levy BD (2005) Cyclooxygenase 2 plays a pivotal role in the resolution of acute lung injury. *J Immunol* 174(8):5033–5039.
16. Mochizuki M, et al. (2005) Role of 15-deoxy delta(12,14) prostaglandin J_2 and Nrf2 pathways in protection against acute lung injury. *Am J Respir Crit Care Med* 171(11): 1260–1266.
17. Spik I, et al. (2005) Activation of the prostaglandin D_2 receptor DP2/CRTH2 increases allergic inflammation in mouse. *J Immunol* 174(6):3703–3708.
18. Teijaro JR, et al. (2011) Endothelial cells are central orchestrators of cytokine amplification during influenza virus infection. *Cell* 146(6):980–991.
19. Levy BD, Clish CB, Schmidt B, Gronert K, Serhan CN (2001) Lipid mediator class switching during acute inflammation: Signals in resolution. *Nat Immunol* 2(7): 612–619.
20. Genovese T, et al. (2005) Effect of rosiglitazone and 15-deoxy-Delta^{12,14}-prostaglandin J_2 on bleomycin-induced lung injury. *Eur Respir J* 25(2):225–234.
21. Rajakariar R, et al. (2007) Hematopoietic prostaglandin D2 synthase controls the onset and resolution of acute inflammation through PGD_2 and 15-deoxyDelta$^{12\ 14}$ PGJ_2. *Proc Natl Acad Sci USA* 104(52):20979–20984.
22. Matsuoka T, et al. (2000) Prostaglandin D_2 as a mediator of allergic asthma. *Science* 287(5460):2013–2017.
23. Mohri I, et al. (2006) Prostaglandin D_2-mediated microglia/astrocyte interaction enhances astrogliosis and demyelination in twitcher. *J Neurosci* 26(16):4383–4393.
24. Satoh T, et al. (2006) Prostaglandin D_2 plays an essential role in chronic allergic inflammation of the skin via CRTH2 receptor. *J Immunol* 177(4):2621–2629.